Emodin reverses resistance to gemcitabine in pancreatic cancer by suppressing stemness through regulation of the epithelial-mesenchymal transition

WEITIAN WEI, JIANGFENG WANG, YUQIAN HU, SHENG CHEN and JINSHI LIU

The Cancer Hospital of the University of Chinese Academy of Sciences (Zhejiang Cancer Hospital), Institute of Cancer and Basic Medicine, Chinese Academy of Sciences, Hangzhou, Zhejiang 310022, P.R. China

Received March 17, 2022; Accepted August 12, 2022

DOI: 10.3892/etm.2022.11706

Abstract. The present study aimed to explore the effects and underlying mechanisms of emodin (Emo) on gemcitabine (GEM)-resistant pancreatic cancer. GEM-resistant SW1990 cells (SW1990/GZ) were established by successively doubling the concentration of GEM. Cell viability was measured using the CCK-8 assay and flow cytometry was used to measure cell apoptosis. Cell migration was assessed using a Transwell assay. Sphere and colony-formation assays were used to evaluate cell self-renewal. The expression levels of epithelial-mesenchymal transition (EMT) and stem cell biomarkers were determined using western blotting. Snail family transcriptional repressor 1 gene (Snail) was overexpressed by transfecting cells with pcDNA3.1-Snail plasmids. A xenograft model was established in nude mice by using SW1990/GZ and Snail-overexpressing SW1990/GZ cells. Proliferation, migration, self-renewal and EMT progression of GEM-treated SW1990/GZ cells were significantly suppressed *in vitro* by Emo treatment, whereas the overexpression of Snail abolished the aforementioned effects. In *in vivo*, the antitumor activity of GEM and the inhibitory effect of GEM against EMT progression and stem-like characteristics were enhanced by treatment with Emo, whilst overexpression of Snail reversed these effects. In conclusion, Emo reversed GEM resistance in pancreatic cancer by suppressing stemness and regulating EMT progression.

Introduction

Pancreatic cancer is a common malignant tumor with almost equivalent morbidity and mortality rates (~15/100,000), and is third leading cause of cancer-related mortality (1). Gemcitabine (GEM) is regarded as the first-line chemotherapy drug for pancreatic cancer treatment (2). However, GEM-resistance in pancreatic cancer significantly shortens progression-free survival in patients treated with GEM (3,4). Cancer stem cells (CSCs) are closely related to GEM-resistance in pancreatic cancer (5-7). CSCs are a subset of cancer cells capable of self-renewal and are involved in the development, metastasis and relapse of pancreatic cancer (8-10). CSCs are present in GEM-resistant pancreatic tumor cells (11) and the process of epithelial-mesenchymal transition (EMT) enhances the migration and invasion of CSCs (6,11). The progression of pancreatic cancer is facilitated by the phenomenon of GEM-resistance that is originating from both CSCs and EMT (7). Therefore, exploring the relative mechanisms of GEM resistance induced by CSCs and EMT is pivotal for the treatment of GEM-resistant pancreatic cancer.

EMT is a necessary step for embryonic development and is involved in multiple physiological and pathological processes, such as injury repair, inflammation, fibrosis and tumorigenesis (12). Cell migration, stem-like characteristics and chemotherapy resistance can be induced by EMT, which further contributes to immune, senescent and apoptotic escape (13). An association between CSCs and EMT has been widely reported. Mani *et al* (14) induced EMT progression in human mammary epithelial cells using EMT transcription factors such as the snail family transcriptional repressor 1 (Snail), the basic helix-loop-helix transcription factor (Twist) or TGF-β1. Following EMT activation, upregulation of stem cell biomarkers, formation of mammary stem cell spheres and soft agar colonies and enhanced tumorigenesis are observed and considered as an indication of CSCs (15). In addition, in stem cells extracted from rodent and human breast epithelium and tumor tissues, a high expression level of the EMT phenotype is observed (16). Therefore, EMT progression and the associated formation of CSCs could be important targets for the treatment of GEM-resistant pancreatic cancer.

Emodin (Emo; 1,3,8-trihydroxy-6-methylanthraquinone) is an anthoquinone derivative extracted from the rhizome of knotweed (*Polygonum cuspidatum*) and rhubarb (*Rheum officinale* baill) and has multiple bioactivities, such as anti-inflammatory, antibacterial, anti-oxidative and

Correspondence to: Dr Jinshi Liu, The Cancer Hospital of the University of Chinese Academy of Sciences (Zhejiang Cancer Hospital), Institute of Cancer and Basic Medicine, Chinese Academy of Sciences, 1 East Banshan Road, Gongshu, Hangzhou, Zhejiang 310022, P.R. China
E-mail: yefeng9725boy@163.com

Key words: emodin, epithelial-mesenchymal transition, pancreatic cancer, gemcitabine, cancer stem cells

antitumor activities (17,18). Emo induces cell apoptosis in paclitaxel-resistant A2780 cells by reducing the expression of apoptotic molecules such as survivin and X-linked inhibitor of apoptosis (19). In addition, Emo significantly inhibits EMT progression in colorectal cancer, cervical cancer and head and neck squamous cells (20-22). The present study aimed to investigate the inhibitory effect of Emo on GEM-resistant pancreatic cancer, as well as the underlying mechanism of action, by exploring the impact of Emo on the growth of CSCs and EMT progression.

Methods and materials

Pancreatic cancer cell lines. Human pancreatic cancer cell line SW1990 was obtained from Combioer Biosciences Co., Ltd. and cultured in DMEM (Procell Life Science & Technology Co., Ltd.) supplemented with 10% fetal bovine serum (FBS; Procell Life Science & Technology Co., Ltd.) at 37˚C with 5% CO_2.

Establishment of gemcitabine-resistant pancreatic cancer cell line (SW1990/GZ). The human pancreatic cancer SW1990 cell line was seeded in six-well plates at a density of $1x10^6$ cells/well and cultured in DMEM for 48 h at 37˚C followed by incubation for 7 days with different concentrations of GEM at 37˚C. Following incubation with GEM, the cell viability was measured using the CCK-8 assay and the GEM IC_{50} value was calculated and further used to incubate SW1990 cells for 24 h. To establish the SW1990/GZ cell line, SW1990 cells were incubated with GEM at 2-fold IC_{50} for 24 h, followed by being replaced with the drug-free medium. Subsequently, cells were incubated until 80% confluent, followed by incubation with GEM at 4-fold IC_{50} for 24 h. The aforementioned procedure was repeated and the incubation concentration of GEM was increased by 2-fold each cycle until the final concentration reached ~1,000 μg/ml, followed by incubation in blank medium for 3 months. Finally, a CCK-8 assay was used to confirm GEM-resistance.

Transmission electron microscope (TEM). Cells were collected following centrifugation at 300 x g at room temperature for 10 min, washed twice with PBS buffer, fixed overnight with 4.0% glutaraldehyde in PBS at 4˚C and then embedded in epoxy resin. Subsequently, ultrathin sections (thickness, 50-70 nm) were cut and collected on copper grids, followed by counterstaining with 3% aqueous uranyl acetate for 1 h at room temperature. Sections were then incubated with 2% phosphotungstic acid for 1 h at room temperature and 1% Reynolds' lead citrate for 20 min at room temperature. Finally, a TEM (JEM-1400Flash; JEOL, Ltd.) was used for examination.

CCK-8 assay. Cell viability was measured using a CCK-8 assay kit (Nanjing Jiancheng Bioengineering Research Institute Co., Ltd.). Cells were seeded in 96-well plates at a density of $1x10^5$ cells/well and incubated at 37˚C for 24 h. Subsequently, 10 μl CCK-8 reagent was added to each well and incubated for 3 h at 37˚C. The absorbance of each was at 450 nm was measured using a microplate reader (PerkinElmer, Inc.) and the IC_{50} value was calculated using GraphPad Prism 8 software (GraphPad Software, Inc.). Finally, the resistant index (RI) was calculated according to the following formula: $RI=IC_{50(SW1990/GZ)}/IC_{50(SW1990)}$.

Sphere formation assay. Cells were centrifuged at 300 x g for 5 min at room temperature, collected and resuspended in PBS Subsequently, $1x10^3$ cells were transferred into each well of a six-well plate and then cultured with serum-free DMEM-F12 medium (Procell Life Science & Technology Co., Ltd.). Following incubation at 37˚C for 7 days, a transparent tape with mesh was overlaid to the bottom of the wells and an inverted microscope (Ts2; Nikon Corporation) was used to count the stem cell spheres.

Colony-formation assay. Cells were seeded in a 6-well plate at a $2x10^2$ cells/well density and incubated for 10 days. Subsequently, the cells were fixed and stained with 6% (w/v) glutaraldehyde and 0.5% crystal violet (Sigma-Aldrich; Merck KGaA) for 60 min at room temperature, followed by washing and air drying at room temperature. Finally, images were captured using an inverted microscope (Olympus, Corporation).

Analysis of apoptosis. Apoptosis of cells was evaluated using a flow cytometry assay. In brief, the cells were seeded in 6-well plates and incubated with 195 μl Annexin V-fluorescein isothiocyanate (Wuhan Punosai Life Technology Co., Ltd.), followed by the addition of 5 μl propidium iodide (BD Biosciences) and incubation for 10 min at room temperature in the dark. Finally, the samples were loaded onto a flow cytometer (BD Bioscience) for apoptosis analysis.

Transwell assay. A total of $1.5x10^5$ cells were plated in the upper chambers of Transwell plates using serum-free DMEM (Corning, Inc.). Complete DMEM supplemented with 20% FBS was added into the lower chamber. Following incubation at 37˚C for 24 h, the migratory cells were stained with 0.1% crystal violet at room temperature for 10 min. Finally, stained cells were counted in 3 random fields using an optical microscope (Ts2; Nikon Corporation).

Transfection. Snail-overexpressing SW1990/GZ cells were established by transfecting the cells implanted in 6-well plates at a density of $1x10^6$ cells/well with pcDNA3.1-Snail (Genscript) using 2 μg Lipofectamine® 2000 (Thermo Fisher Scientific, Inc.). pcDNA3.1-NC (Genscript) was used as the negative control. After incubation for 48 h at 37˚C, transfection efficacy was measured through western blot analysis.

Western blot assay. Total protein from cells was extracted using RIPA Lysis Buffer (Sigma-Aldrich; Merck KGaA) and quantified using a BCA kit (Sigma-Adrich; Merck KGaA). Total protein (~30 μg/lane) was separated utilizing SDS-PAGE on a 12% gel and subsequently transferred onto a PVDF membrane. The membrane was blocked with 5% BSA (Beyotime Institute of Biotechnology) at room temperature for 2 h to remove non-specific binding proteins, followed by incubation with primary antibodies against CD44 (1:800; cat. no. DF6392; Affinity Biosciences, Ltd.), Aldehyde dehydrogenase 1 (ALDH1; 1:1,000; cat. no. DF6625; Affinity

Biosciences, Ltd.), Nanog (1:1,000; cat. no. AF5388; Affinity Biosciences, Ltd.), E-cadherin (1:800; cat. no. AF0131; Affinity Biosciences, Ltd.), vimentin (1:1,000; cat. no. AF7013; Affinity Biosciences, Ltd.), Snail (1:1,000; cat. no. AF6032; Affinity Biosciences, Ltd.) and GAPDH (1:5,000; cat. no. AF7021; Affinity Biosciences, Ltd.) at 4˚C for 12 h. The membrane was then washed and incubated with the anti-rabbit IgG HRP-linked secondary antibody (1:3,000, cat. no. 7074, CST Biological Reagents Co., Ltd.) at room temperature for 1.5 h. Finally, the membrane was incubated with ECL solution (Beyotime Institute of Biotechnology) and exposed to a Tanon 5200-multi (Tanon Science and Technology Co., Ltd.). The relative expression levels of the target proteins were quantified using ImageJ 1.8.0.172 software (National Institutes of Health) with GAPDH as the loading control.

Xenograft experiments. A total of 18 5-6-week-old male SPF BABL/c nude mice weighing 16-20 g were purchased from Shanghai Lingchang Biological Technology Co., Ltd. Animals were housed in individually ventilated cages (Suzhou Suhang Technology Equipment Co., Ltd.) at 20-24˚C, 40-60% humidity, minimum air change rate of 15/h, minimum pressure gradient of 10 Pa, ammonia concentration ≤14 mg/m^2, noise ≤60 db, 12-h light/dark cycle and with *ad libitum* access to food and water.

For the *in vivo* experiment, six groups were used: GEM + Snail OE + EmoControl, Snail OE, GEM, GEM + Snail OE, GEM + Emo, and GEM + Snail OE + Emo. For the general procedure of xenograft model establishment, 1x10^7 cells were subcutaneously injected into the axilla of each mouse. Animals in the control group were xenografted with SW1990/GZ cells, followed by intraperitoneal injection with an equal volume of normal saline. In the Snail OE group, animals were xenografted with Snail-overexpressing SW1990/GZ cells, followed by intraperitoneal injection with an equal volume of normal saline. The animals in the GEM and GEM + Snail OE groups, nude mice were injected with SW1990/GZ cells and Snail-overexpressing SW1990/GZ cells, respectively, followed by intraperitoneal injection with 60 mg/kg GEM at a volume of 10 ml/kg. Animals in the GEM + Emo and GEM + Snail OE + Emo groups were xenografted with SW1990/GZ cells and Snail-overexpressing SW1990/GZ cells, respectively, followed by intraperitoneal injection of 60 mg/kg GEM and subcutaneous injection of 1 mg/kg Emo at a volume of 10 ml/kg (23). A total of three mice were used for each group. All administrations were initiated when the tumor volume reached 100 mm^3. GEM was administered on days 1, 4, 7, 10, 14 and 16, whereas Emo was administered daily. Tumor volume was measured and calculated using the following formula: V=LxW^2/2, where V represents volume in mm^3, L represents the greatest diameter in mm and W represents the lowest diameter in mm. The animals were euthanized using the method of CO_2 euthanasia and then the tumors were explanted, weighed and images captured.

H&E staining. The tumor tissues were collected, washed with sterile water for 2 h and dehydrated with 70, 80 and 90% ethanol series. Subsequently, the tissues were incubated with equal quality ethanol and xylene for 15 min, and then incubated with xylene of equal quality for another 15 min. This incubation procedure was repeated until the tissues were cleared. Finally, the tissues were embedded in paraffin, sectioned at a 5-mm thickness and stained with H&E. Finally, tissues were observed in five randomly-selected fields under an inverted microscope (Olympus Corporation), with images captured.

Immunohistochemical assay. Tissue sections were deparaffinized by rinsing with xylene for 10 min, followed by hydration using a 2-min incubation with absolute ethyl alcohol, 95% ethyl alcohol, 85% ethyl alcohol and 75% ethyl alcohol, successively. Sections were rinsed with PBS and incubated with endogenous peroxidase blocking solution (P0100A; Beyotime Institute of Biotechnology) at room temperature for 10 min, followed by incubation with 10% goat serum (Gibco; Thermo Fisher Scientific, Inc.) blocking solution at room temperature for 2 h. Specimens were then incubated with primary antibodies against E-cadherin (1:10; cat. no. ab231303; Abcam), vimentin (1:50; cat. no. ab20346; Abcam), Snail (1:50; cat. no. AF6032; Affinity Biosciences, Ltd.), Nanog (1:100; cat. no. 14295-1-AP; Proteintech Group, Inc.; Wuhan Sanying Biotechnology), CD44 (1:100, 15675-1-AP, Proteintech Group, Inc.; Wuhan Sanying Biotechnology), or ALDH1 (1:100, 15910-1-AP, Proteintech Group, Inc.; Wuhan Sanying Biotechnology) at 4˚C for 24 h, followed by washing with PBS. Following primary antibody incubation, the tissues were incubated with the goat anti-rabbit IgG H&L (HRP) preadsorbed secondary antibody (1:100; cat. no. ab97080; Abcam) was added and incubated at 4˚C for 24 h, followed by rinsing and staining with 3,3'-diaminobenzidine dye (MilliporeSigma). Finally, images were captured using an inverted light microscope (Eclipse E100; Nikon Corporation).

Ethics statements. All animal experiments performed in this study were authorized by the ethical committee of Zhejiang Cancer Hospital (approval no. 2019-07-006) and conducted according to the guidelines for care and use of laboratory animals and the principles of laboratory animal care and protection.

Statistical analysis. Statistical analysis was performed using SPSS (version 25.0; IBM Corp.). The Kruskal-Wallis test was used for unequal distribution of tumor weights and single comparisons were performed using the Mann-Whitney test. For analysis on other data, one-way ANOVA followed by Tukey's post hoc test was applied. $P<0.05$ was considered to indicate a statistically significant difference.

Results

GEM-resistant SW1990 (SW1990/GZ) cell line is successfully established. SW1990/GZ cell line was successfully established by treating SW1990 cells with increasing concentrations of GEM as confirmed using the CCK-8 assay. Compared with that of SW1990 cells, IC_{50} of GEM changed from 0.04 to 115.6 μg/ml, with a ~3,000-fold increase (Fig. 1).

Emo significantly enhances the inhibitory effect of GEM on the self-renewal of SW1990/GZ cells. A total of 6 groups were used to explore the *in vitro* antitumor effects of Emo: SW1990 (naïve SW1990 cells treated with blank medium), SW1990/GZ

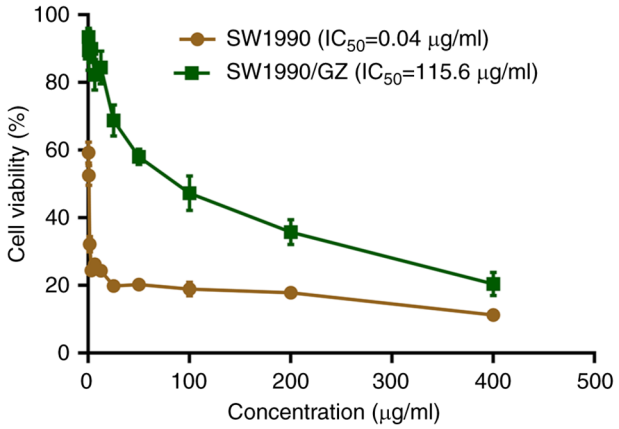

Figure 1. Establishment of gemcitabine-resistant SW1990 cells. CCK-8 cell viability assay and IC_{50} values.

(SW1990/GZ cells incubated with blank medium), GEM + SW1990/GZ (SW1990/GZ cells incubated with 0.04 μg/ml GEM), 20 μM Emo + GEM + SW1990/GZ (SW1990/GZ cells incubated with 0.04 μg/ml GEM and 20 μM Emo), 40 μM Emo + GEM + SW1990/GZ (SW1990/GZ cells incubated with 0.04 μg/ml GEM and 40 μM Emo) and 80 μM Emo + GEM + SW1990/GZ (SW1990/GZ cells incubated with 0.04 μg/ml GEM and 80 μM Emo). The cellular morphology of each group is shown in Fig. 2A. Compared with the SW1990 cells (Fig. 2B), atypical nuclei, large nucleoli and organelle hypertrophy were observed in the SW1990/GZ, GEM + SW1990/GZ and 20 μM Emo + GEM + SW1990/GZ groups, which were dramatically ameliorated by the introduction of 40 and 80 μM Emo, indicating that the malignancy of SW1990/GZ cells was significantly inhibited by GEM in the presence of 40 and 80 μM Emo.

The self-renewal of SW1990/GZ cells was further investigated by using sphere formation and colony-formation assays. Compared with the SW1990 group, the cell sphere-forming rate increased from 31.9 to 38.2% in the SW1990/GZ group, which further declined to 32.1% after treatment with GEM, with no significant difference (P<0.05 vs. SW1990; Fig. 2C). Compared with the GEM + SW1990/GZ group, the cell sphere-forming rate was suppressed to 30.2, 15.4 and 7.5% by co-treatment with 20, 40 and 80 μM Emo, respectively (P<0.01 vs. GEM + SW1990/GZ; Fig. 2C). In addition, the number of spheres was significantly greater in the SW1990/GZ group than that in the SW1990 group (P<0.05 vs. SW1990; Fig. 2D). After the introduction of 40 μM and 80 μM Emo, the number of spheres decreased significantly (P<0.01 vs. GEM + SW1990/GZ; Fig. 2D). The expression levels of stem cell biomarkers were determined through western blot analysis. Compared with SW1990 cells, the expression levels of CD44, ALDH1, Nanog and Snail were significantly increased in SW1990/GZ cells (P<0.05 vs. SW1990; Fig. 2E). After the introduction of 20, 40 and 80 μM Emo, the expression levels of CD44, ALDH1, Nanog and Snail were decreased (P<0.05 vs. and P<0.01 vs. GEM + SW1990/GZ; Fig. 2E).

Inhibitory effect of GEM on the proliferation, metastasis and EMT progression of SW1990/GZ cells is enhanced by Emo. The apoptotic rate in the SW1990, SW1990/GZ and GEM + SW1990/GZ groups was 10.48, 10.49 and 10.46%, respectively (Fig. 3A). Compared with the GEM + SW1990/GZ group, the apoptotic rate increased to 11.37, 16.61 and 22.45% after co-treatment with 20, 40 and 80 μM Emo, respectively (P<0.01 vs. GEM + SW1990/GZ). In addition, no significant difference in the number of migrated cells was observed among the SW1990, SW1990/GZ, GEM + SW1990/GZ and 20 μM Emo + GEM + SW1990/GZ groups. Compared with the GEM + SW1990/GZ group, the number of migrated cells decreased with the co-introduction of 40 and 80 μM Emo (P<0.01 vs. GEM + SW1990/GZ). No significant differences in cell viability were observed among the SW1990, SW1990/GZ, GEM + SW1990/GZ and 20 μM Emo + GEM + SW1990/GZ groups (Fig. 3C). After treatment with 40 and 80 μM Emo, cell viability was significantly reduced (P<0.01 vs. GEM + SW1990/GZ). Finally, expression levels of the EMT biomarkers were measured. Compared with the SW1990 group, E-cadherin was significantly downregulated and vimentin was significantly upregulated in the SW1990/GZ group (Fig. 3D). Compared with the GEM + SW1990/GZ group, E-cadherin expression was upregulated, while vimentin was downregulated by co-treatment with 20, 40 and 80 μM Emo, respectively (P<0.05 vs. SW1990; P<0.05 vs. GEM + SW1990/GZ; P<0.01 vs. GEM + SW1990/GZ).

Emo represses self-renewal and EMT progression of SW1990/GZ cells. Compared with SW1990/GZ cells, significantly decreased cell sphere-forming rate and number of spheres were observed in 80 μM Emo-treated SW1990/GZ cells (Fig. S1A and B). Furthermore, compared with the SW1990/GZ cells, significantly lower expression of CD44, ALDH1, Nanog and Snail was observed with 80 μM Emo-treated SW1990/GZ cells (P<0.05 vs. SW1990/GZ; Fig. S1C). However, no significant changes were observed in the apoptotic rate (Fig. S1D) and the number of migrated cells (Fig. S1E) after treatment with 80 μM Emo. Compared with SW1990/GZ cells, upregulated E-cadherin and downregulated vimentin (Fig. S1F) were observed in 80 μM Emo-treated SW1990/GZ cells (P<0.05 and P<0.01 vs. SW1990/GZ).

Snail overexpression abolishes the effects of Emo on self-renewal of GEM-treated SW1990/GZ cells. SW1990/GZ cells overexpression Snail were constructed to explore the potential mechanism underlying the effects of Emo. Firstly, the successfully establishment of Snail-overexpressed SW1990/GZ cells was verified by Western blotting assay, which was shown in Fig. S2. Six groups were compared: Control (SW1990/GZ cells cultured in blank medium), Snail OE (Snail-overexpressed SW1990/GZ cells cultured in blank medium), GEM (SW1990/GZ cells treated with 0.04 μg/ml GEM), GEM + Snail OE (Snail-overexpressed SW1990/GZ cells treated with 0.04 μg/ml GEM), GEM + Emo (SW1990/GZ cells treated with 0.04 μg/ml GEM and 80 μM Emo) and GEM + Snail OE + Emo (Snail-overexpressed SW1990/GZ cells treated with 0.04 μg/ml GEM and 80 μM Emo).

Compared with the control, Snail was significantly upregulated in the Snail OE group, indicating the successful establishment of Snail-overexpressing SW1990/GZ cells (P<0.05 vs. control; Fig. 4A). Compared with the GEM group, Snail was significantly upregulated in the GEM + Snail OE

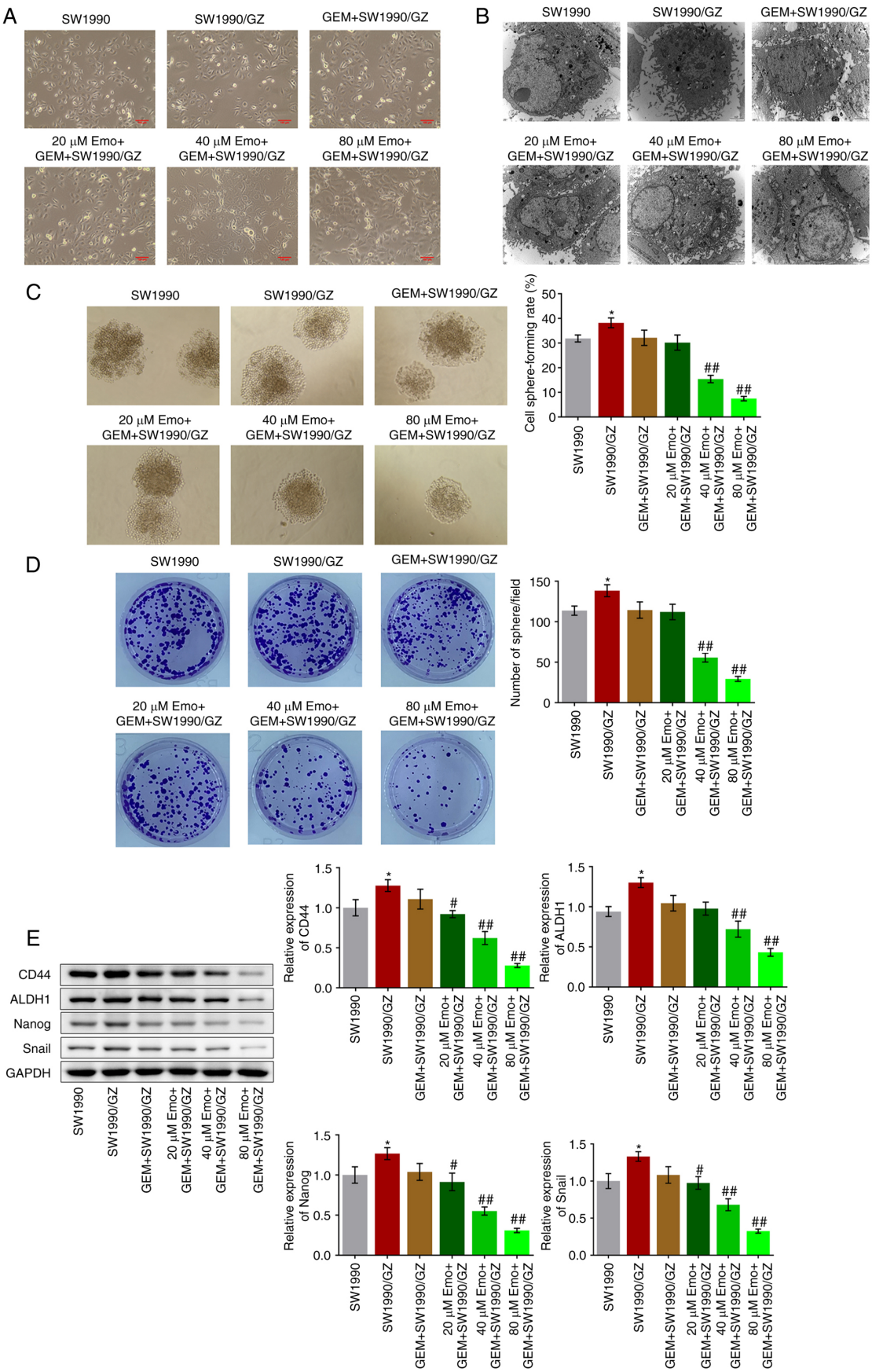

Figure 2. Emo enhances inhibitory effects of GEM on self-renewal of SW1990/GZ cells. (A) Morphology of cells observed under an inverted light microscope (scale bar, 100 μm). (B) The ultrastructure of cells observed under a transmission electron microscope (x10,000 magnification). (C) Cell sphere-forming rate evaluated using the sphere formation assay (x100 magnification). (D) Number of spheres measured using the colony-formation assay (x200 magnification). (E) Expression levels of CD44, ALDH1, Nanog and Snail determined using western blotting assays. *P<0.05 vs. SW1990. #P<0.05 vs. GEM + SW1990/GZ. ##P<0.01 vs. GEM + SW1990/GZ. Emo, emodin; GEM, gemcitabine; SW1990/GZ, GEM-resistant SW1990 cells; ALDH1, Aldehyde dehydrogenase 1; Snail, Snail family transcriptional repressor 1 gene.

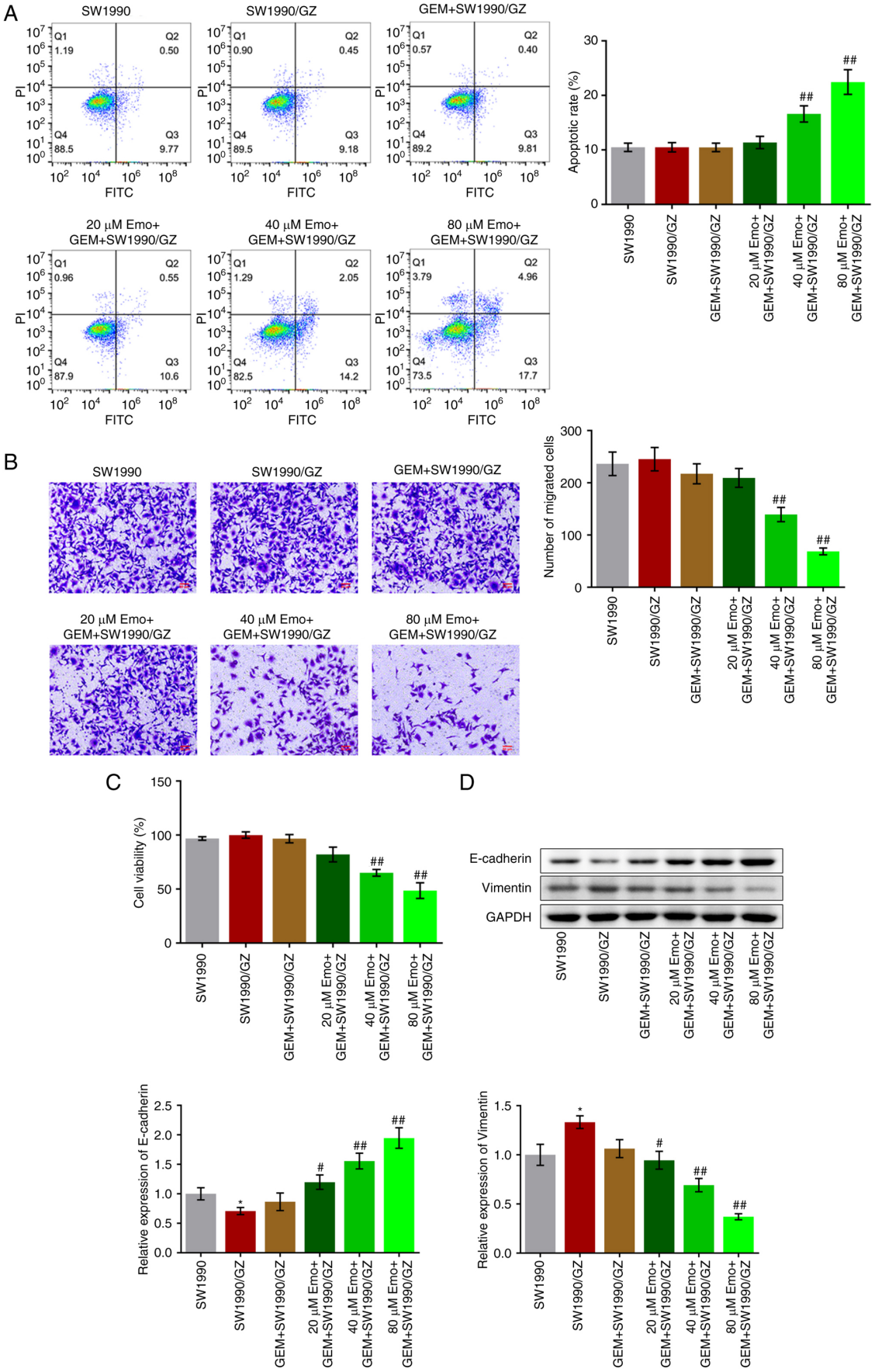

Figure 3. Emo enhances inhibitory effects of GEM on cell proliferation, migration and EMT progression of SW1990/GZ cells. (A) Flow cytometry assay for the analysis of cell apoptosis. (B) Cell migration measured via Transwell assay (scale bar, 50 μm). (C) CCK-8 cell viability assay. (D) Western blotting assay used to determine the expression level of vimentin and E-cadherin. *P<0.05 vs. SW1990. $^{\#}$P<0.05 vs. GEM + SW1990/GZ. $^{\#\#}$P<0.01 vs. GEM + SW1990/GZ. Emo, emodin; GEM, gemcitabine; SW1990/GZ, GEM-resistant SW1990 cells; EMT, epithelial-mesenchymal transition; ALDH1, Aldehyde dehydrogenase 1; Snail, Snail family transcriptional repressor 1 gene.

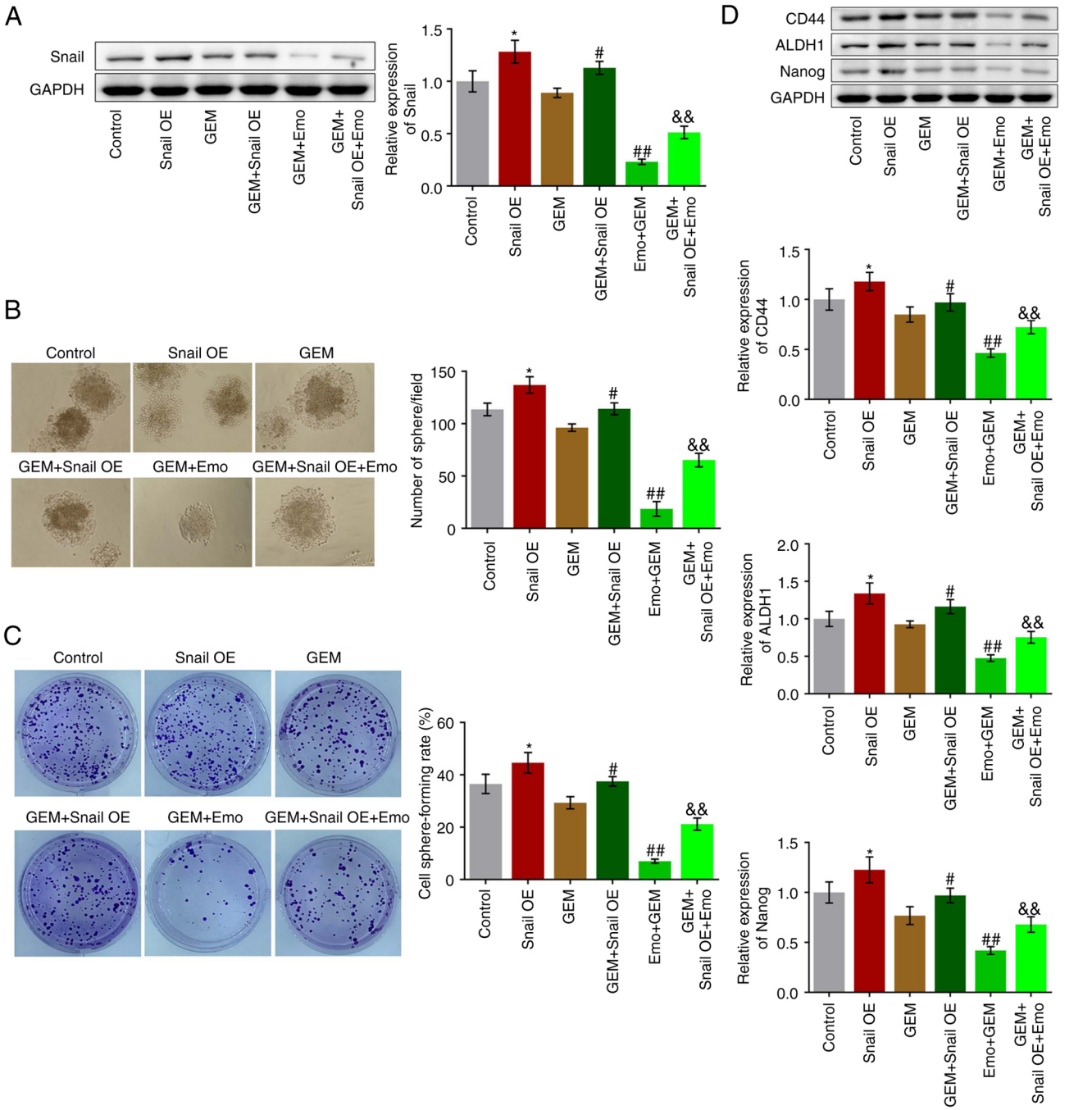

Figure 4. Effects of emodin on the self-renewal of GEM-treated SW1990/GZ cells is abolished by Snail overexpression. (A) Expression level of Snail determined via western blotting assay. (B) Cell sphere-forming rate evaluated using the sphere formation assay (x100 magnification). (C) Number of spheres measured using the colony-formation assay (x200 magnification). (D) Expression levels of CD44, ALDH1 and Nanog measured using western blotting assay. *P<0.05 vs. control. #P<0.05 vs. GEM. ##P<0.01 vs. GEM. &&P<0.01 vs. Emo + GEM. GEM, gemcitabine; SW1990/GZ, GEM-resistant SW1990 cells; ALDH1, Aldehyde dehydrogenase 1; Snail, Snail family transcriptional repressor 1 gene; Snail OE, Snail overexpression.

group and downregulated in the Emo + GEM group, while Snail was significantly upregulated in the GEM + Snail OE + Emo group compared with the Emo + GEM group (P<0.05 and P<0.01 vs. GEM group; P<0.01 vs. Emo + GEM). Compared with the control, the cell sphere-forming rate was significantly elevated from 36.5 to 44.6% in the Snail OE group (P<0.05; Fig. 4B). Compared with the GEM group, the cell sphere-forming rate was increased from 29.3 to 37.5% in the GEM + Snail OE group and decreased from 29.3 to 7.01% in the Emo + GEM group, while was further increased to 21.20% in the Emo + Snail OE + GEM group (P<0.05 vs. control; P<0.05 vs. GEM; P<0.01 vs. GEM; P<0.01 vs. Emo + GEM: Fig. 4B). In addition, compared with the control, the number of spheres dramatically increased in the Snail OE group (P<0.05; Fig. 4C). Compared with the GEM group, the number of spheres was increased in the GEM + Snail OE group and decreased in the Emo + GEM group, which was further increased in the GEM + Snail OE + Emo group compared with the Emo + GEM group (P<0.05 vs. GEM; P<0.01 vs. GEM; P<0.01 vs. Emo + GEM: Fig. 4C).

Finally, the expression levels of the stem cell biomarkers were determined. Compared with the control, CD44, ALDH1 and Nanog were significantly upregulated in the Snail OE group (P<0.05; Fig. 4D). Compared with the GEM group, CD44, ALDH1 and Nanog were significantly upregulated in the GEM + Snail OE group, downregulated in the Emo + GEM group, while was further upregulated in the Emo + Snail OE + GEM group compared with the Emo + GEM group (P<0.05 vs. GEM; P<0.01 vs. GEM; P<0.01 vs. Emo + GEM; Fig. 4D).

Snail overexpression abolishes the effect of Emo on proliferation, metastasis and EMT progression in GEM-treated SW1990/GZ cells. The apoptotic rate significantly decreased from 11.65 to 6.26% in the Snail OE group (P<0.05; Fig. 5A), while it was increased to 13.74% in GEM group (Fig. 5A). Compared with the GEM group, no significant difference was observed in the apoptotic rate in the GEM + Snail OE group and the apoptotic rate was significantly increased to 22.66% in the Emo + GEM group, while it was further decreased to 16.29% in the Emo + Snail OE + GEM group compared with the Emo + GEM group (P<0.01 vs. GEM; P<0.01 vs. Emo + GEM). In addition, compared with the control, the number of migrated cells was significantly increased in the Snail OE group (P<0.05 vs. control; Fig. 5B). Compared with the GEM group, the number of migrated cells was slightly increased in the GEM + Snail OE group and decreased in the Emo + GEM group, while it was significantly elevated in the GEM + Snail OE + Emo group compared with the Emo + GEM group (P<0.01 vs. GEM; P<0.01 vs. Emo + GEM). No significant difference in cell viability was observed among the control, Snail OE, GEM and GEM + Snail OE groups. Compared with the GEM group, cell viability was significantly reduced in the Emo + GEM group, which while it was significantly increased in the Emo + Snail OE + GEM group compared with the Emo + GEM group (P<0.01 vs. GEM; P<0.01 vs. Emo + GEM; Fig. 5C). Finally, the expression levels of the EMT biomarkers were evaluated. Compared with the control, E-cadherin was significantly downregulated and vimentin was significantly upregulated in the Snail OE group (P<0.05; Fig. 5D). Compared with the GEM group, the expression level of E-cadherin was significantly decreased and that of vimentin was significantly increased in the GEM + Snail OE group. Compared with the GEM group, the expression levels of E-cadherin and vimentin were significantly increased and decreased, respectively, while the expression levels of E-cadherin and vimentin were significantly decreased and increased, respectively, in the Emo + Snail OE + GEM group compared with the Emo + GEM group (P<0.05 and P<0.01 vs. GEM; P<0.01 vs. Emo + GEM).

Snail overexpression abolishes the enhancement of Emo on the anti-tumor efficacy of GEM on SW1990/GZ xenograft model. To verify the effects of Emo on the anti-tumor efficacy of GEM against GEM-resistant pancreatic cancer, a xenograft model in nude mice with SW1990/GZ cells or Snail-overexpressing SW1990/GZ cells was established. After 16 days of treatments, tumor volume and weight were significantly increased in the Snail OE group compared with control (Fig. 6A-C). Compared with the GEM group, tumor volume and weight were significantly increased in the GEM + Snail OE group and decreased in the Emo + GEM group, which were significantly reversed in the Emo + Snail OE + GEM group. Furthermore, H&E staining (Fig. 6D) was used to evaluate the pathological state of the tumor tissues. No significant differences were observed between the control and Snail OE groups. However, compared with the GEM group, the H&E score was greatly reduced in the GEM + Snail OE group and elevated in the Emo + GEM group, which was dramatically rescued in the Emo + Snail OE + GEM group. (P<0.05 vs. control; P<0.01 vs. control; P<0.05 vs. GEM; P<0.01 vs. GEM; P<0.05 vs. Emo + GEM; P<0.01 vs. Emo + GEM).

Snail overexpression abolishes the inhibitory effect of Emo against stem cell growth and EMT progression in SW1990/GZ xenograft model. Tumor tissues were homogenized for western blotting analysis and tissue sections were utilized for immunohistochemical assays. Compared with the control, the expression levels of CD44, ALDH1, Nanog and Snail were significantly elevated in the Snail OE group (P<0.05 vs. control; Fig. 7A and B). Compared with the GEM group, CD44, ALDH1, Nanog and Snail were significantly upregulated in the GEM + Snail OE group and downregulated in the Emo + GEM group, which was reversed in the Emo + Snail OE + GEM group (P<0.05 and P<0.01 vs. GEM; P<0.05 vs. Emo + GEM; P<0.01 vs. Emo + GEM). These data indicate that the stem-like symptoms in SW1990/GZ tumors were significantly alleviated by Emo by inactivating Snail. In addition, compared with the control, the expression level of E-cadherin was decreased and that of vimentin was increased in the Snail OE group (P<0.05; Fig. 7C and D). Compared with the GEM group, E-cadherin was downregulated and vimentin was upregulated in the GEM + Snail OE group and E-cadherin was upregulated and vimentin was downregulated in the Emo + GEM group, while it was significantly reversed in the Emo + Snail OE + GEM group compared to the Emo + GEM group (P<0.05 and P<0.01 vs. GEM; P<0.05 and P<0.01 vs. Emo + GEM).

Discussion

Resistance to chemotherapy is an important barrier in the clinical treatment of pancreatic cancer (24). CSC-like characteristics in pancreatic tumor cells, which contribute to chemotherapy resistance, tumorigenesis, tumor relapse and metastasis have been shown in multiple reports (25-27). In addition, similar biofunctions are observed between CSCs and tumor cells with EMT phenotypes, which are reported to be involved in the development and progression of chemotherapy resistance, tumor relapse and metastasis (7). In the present study, GEM-resistant pancreatic tumor cells were established in SW1990 cells by successively doubling the concentration of GEM, which was verified by the increased IC_{50} against GEM in a 3,000-fold manner. In addition, the resistance of SW1990/GZ cells to GEM was accompanied by enhanced self-renewal and EMT progression, which was consistent with a previous report (28).

Pancreatic circulating tumor cells enter the circulatory system to achieve EMT phenotypes and their migration is significantly enhanced. Rhim *et al* (29) report that in pancreatic

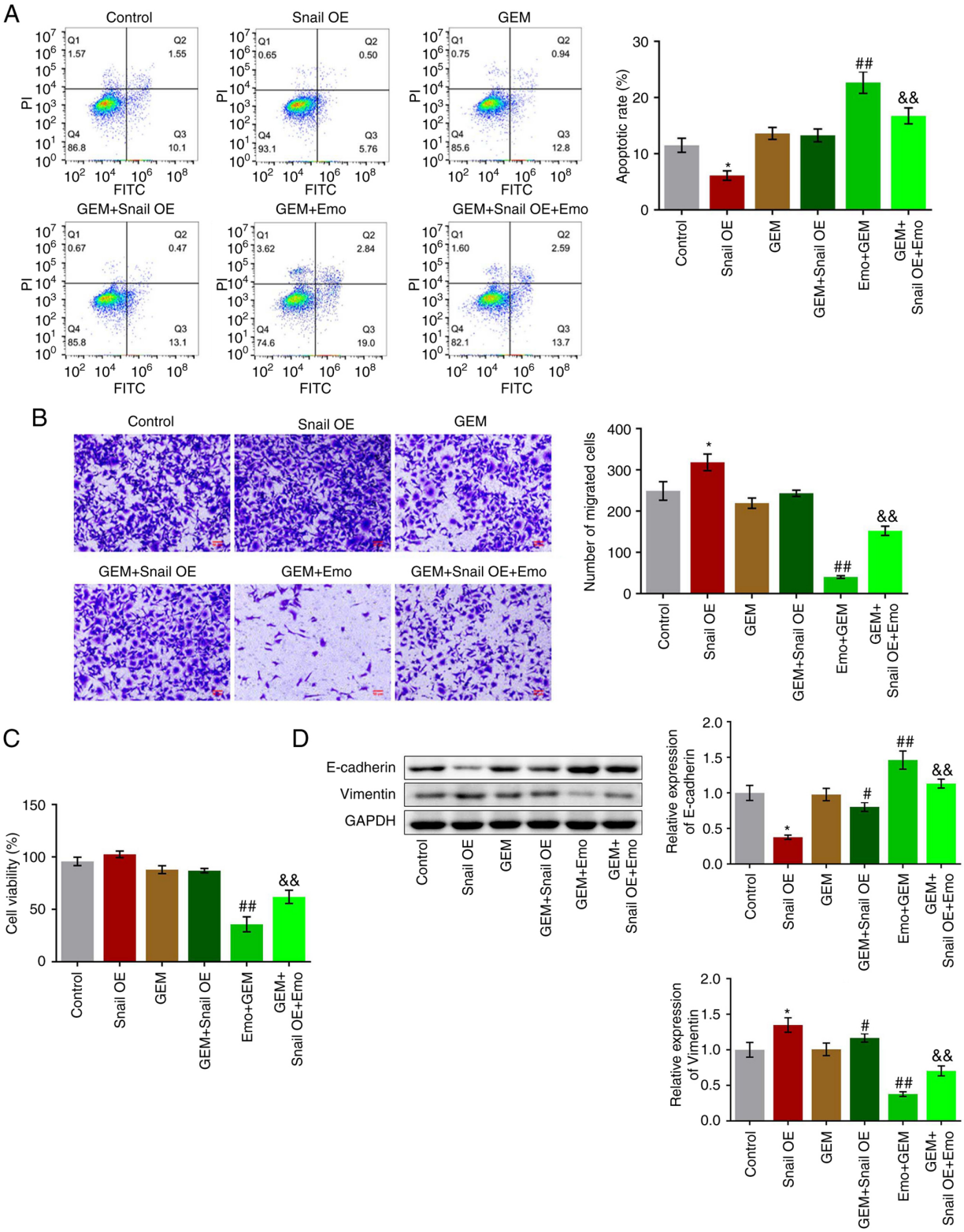

Figure 5. Effects of Emo on the proliferation, metastasis and EMT progression in GEM-treated SW1990/GZ cells is abolished by Snail overexpression. (A) Flow cytometry assay for the analysis of cell apoptosis. (B) Cell migration via Transwell assay (scale bar, 50 μm). (C) CCK-8 cell viability assay. (D) Expression level of vimentin and E-cadherin via western blotting. *P<0.05 vs. control. $^{\#}$P<0.05 vs. GEM. $^{\#\#}$P<0.01 vs. GEM. $^{\&\&}$P<0.01 vs. Emo + GEM. Emo, emodin; GEM, gemcitabine; SW1990/GZ, GEM-resistant SW1990 cells; Snail, Snail family transcriptional repressor 1 gene; EMT, epithelial-mesenchymal transition; Snail OE, Snail overexpression.

circulating tumor cells, the number of $CD24^{+}CD44^{+}$ cells is ~100-fold higher compared with that in pancreatic tumor tissues, indicating that stem-like characteristics are observed in tumor cells with EMT phenotypes. It has been reported that in isolated $CD24^{+}CD44^{+}$ pancreatic tumor cells, significant resistance against GEM is observed, accompanied by upregulation of EMT phenotypes (25). Voon *et al* (30) induced EMT phenotypes in GIF-14 rodent gastric epithelial cells

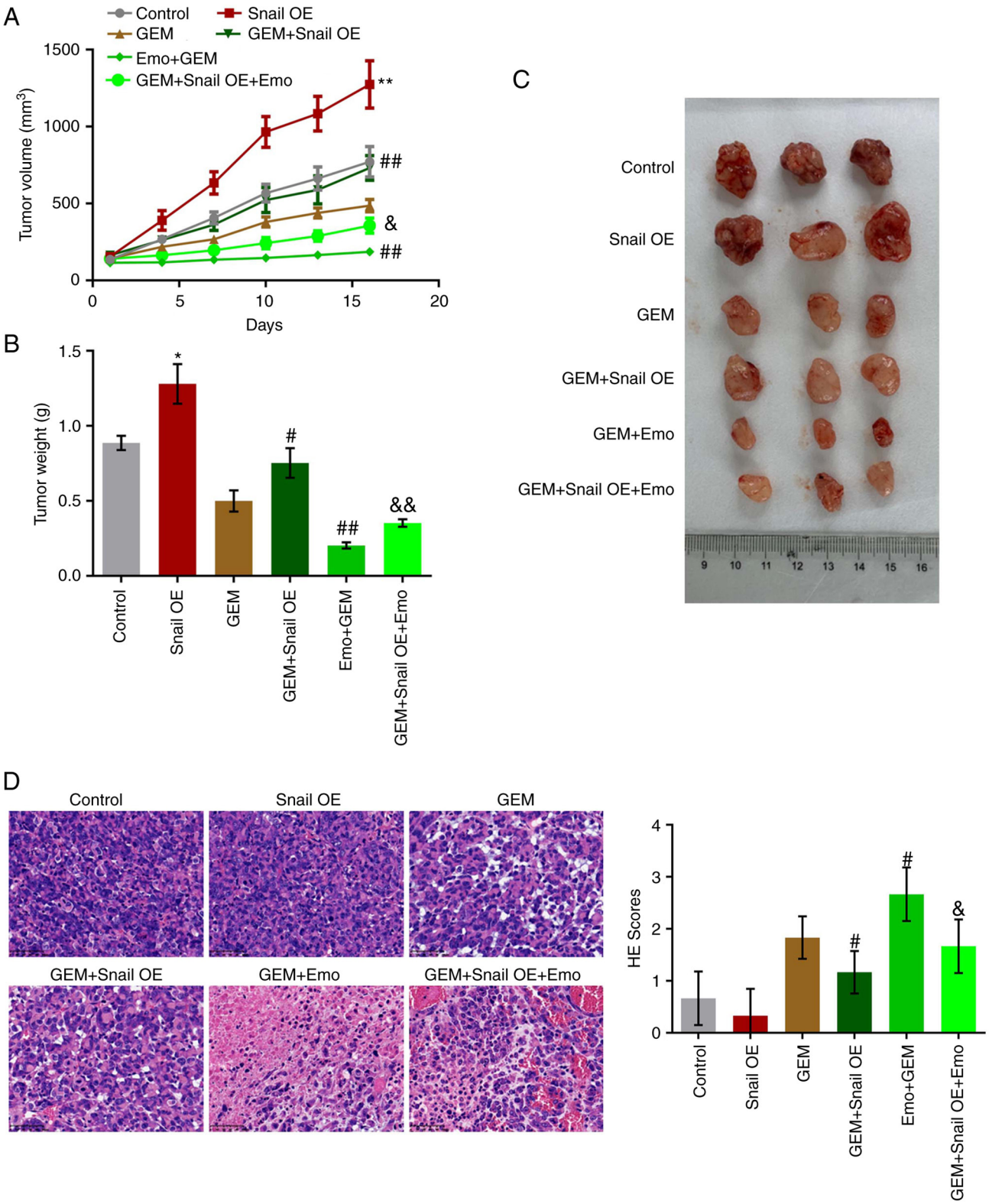

Figure 6. Antitumor efficacy of GEM on the SW1990/GZ xenograft model is enhanced by Emo by inactivating Snail. (A) Tumor volume was recorded during the treatments after 1, 4, 7, 10, 14 and 16 days. (B) Tumor weights as recorded at the end of the animal experiment. (C) Representative picture of tumors taken at the end of the animal experiment. (D) H&E staining utilized to evaluate the pathological state in tumor tissues (x200 magnification). *P<0.05 vs. control. **P<0.01 vs. control. $^{\#}$P<0.05 vs. GEM. $^{\#\#}$P<0.01 vs. GEM. $^{\&}$P<0.05 vs. Emo + GEM. $^{\&\&}$P<0.01 vs. Emo + GEM). Emo, emodin; GEM, gemcitabine; SW1990/GZ, GEM-resistant SW1990 cells; Snail OE, Snail overexpression.

using TGF-β1 by activating the EGFR/RAS pathway and found that the expression level of the stem cell biomarker leucine-rich repeat-containing G-protein coupled receptor 5 was significantly elevated, accompanied by enhanced sphere and colony-formation. In the present study, Emo treatment significantly enhanced the inhibitory effect of GEM against the

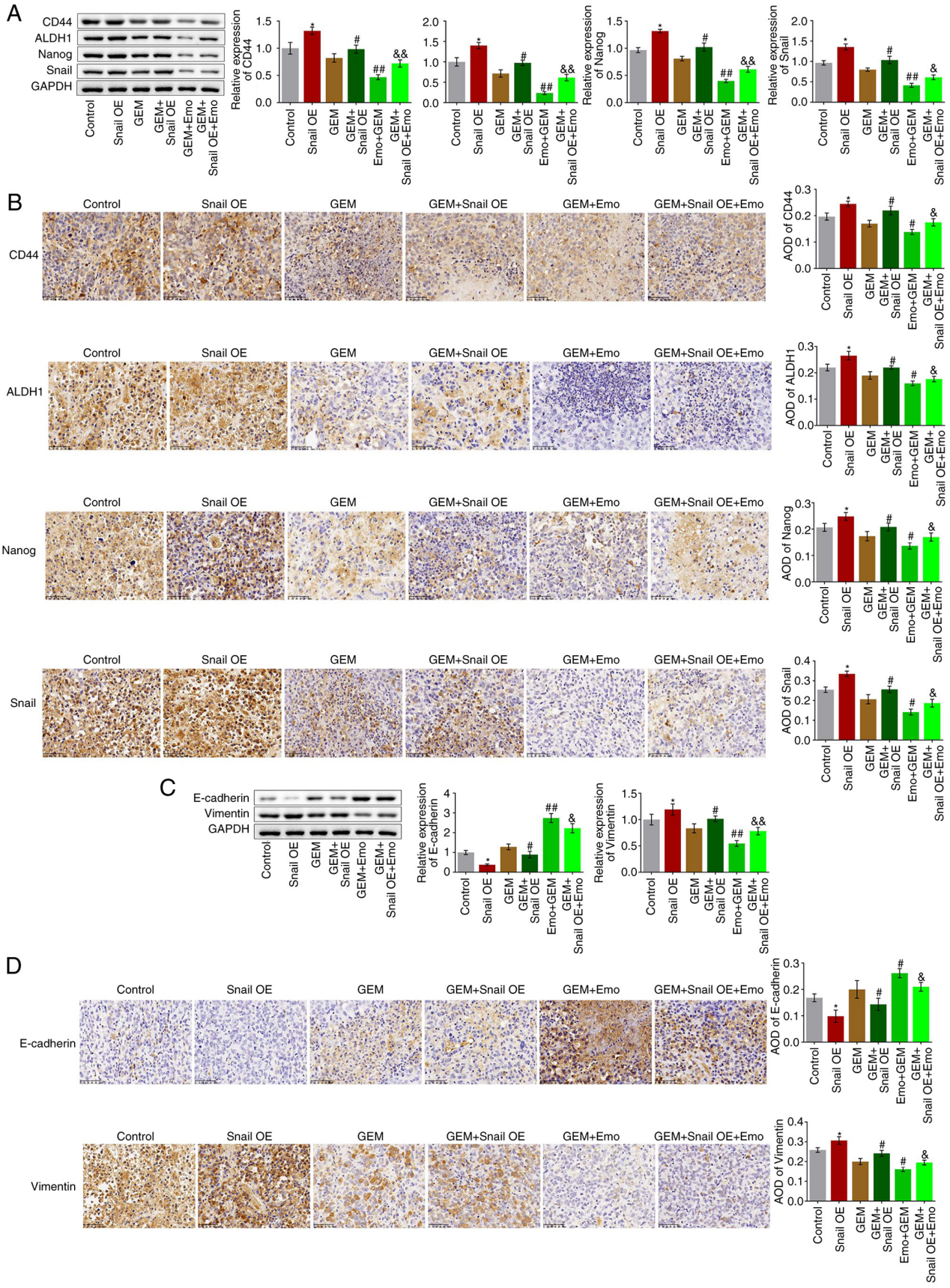

Figure 7. Growth of stem cells and EMT progression in SW1990/GZ xenograft model is inhibited by Emo by inactivating Snail. (A) Expression levels of CD44, ALDH1, Nanog and Snail as determined via western blotting. (B) Expression level of CD44, ALDH1, Nanog and Snail in tumor tissues measured via immunohistochemistry (x200 magnification). (C) Expression levels of vimentin and E-cadherin as determined via western blotting. (D) Expression levels of vimentin and E-cadherin in tumor tissues measured via immunohistochemistry (x200 magnification). *P<0.05 vs. control. $^{\#}$P<0.05 vs. GEM. $^{\#\#}$P<0.01 vs. GEM. $^{\&}$P<0.05 vs. Emo + GEM. $^{\&\&}$P<0.01 vs. Emo + GEM. Emo, emodin; GEM, gemcitabine; SW1990/GZ, GEM-resistant SW1990 cells; Snail, Snail family transcriptional repressor 1 gene; EMT, epithelial-mesenchymal transition; ALDH1, Aldehyde dehydrogenase 1; Snail, Snail family transcriptional repressor 1 gene; Snail OE, Snail overexpression.

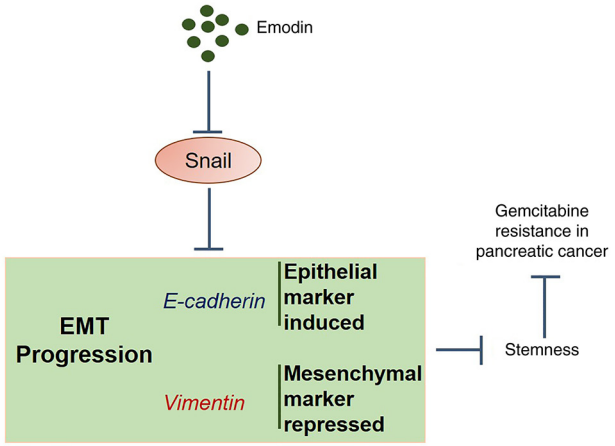

Figure 8. Schematic diagram. Emodin reversed resistance to gemcitabine in pancreatic cancer by suppressing stemness via the regulation of EMT and the inhibition of Snail. EMT, epithelial-mesenchymal transition.

proliferation and migration of SW1990/GZ cells, accompanied by suppressed stem-like and EMT phenotypes, indicating that Emo might reverse the GEM resistance of SW1990/GZ cells by inhibiting the formation of CSCs and the progression of EMT. *In vivo* experiments further confirmed the role of Emo as enhancer of the anti-tumor effect of GEM against GEM-resistant SW1990/GZ xenografts, accompanied by the inhibition of stem-like and EMT phenotypes in tumor tissues, which was consistent with the results observed in the *in vitro* assays.

In the progression of EMT, the expression of biomarkers is regulated by several transcriptional factors, such as Snail, Twist and Zeb, among which Snail is an important transcriptional factor originally discovered in Drosophila melanogaster and proved to be the basis for mesoderm formation (31). By directly binding to the E-box sequence on the promoter of E-cadherin, Snail suppresses EMT progression by inhibiting E-cadherin transcription (32). Xiong *et al* (33) claimed a significant role in regulating EMT progression in pancreatic CSCs (33). In the present study, Snail-overexpressing SW1990/GZ cells were established. These cells showed enhanced proliferation, migration, self-renewal and EMT progression, in agreement with previous results (34,35). By comparing the results of Emo-treated SW1990/GZ cells and Emo-treated Snail-overexpressing SW1990/GZ cells it was found that the reverse effects of Emo against GEM-resistant pancreatic cancer were significantly abolished by the overexpression of Snail *in vitro* and *in vivo*, indicating that Emo enhanced the anti-tumor efficacy of GEM against GEM-resistant pancreatic cancer by downregulating Snail. However, some findings in the present study require further investigation. For example, compared with the control, the cell proliferation and migration were significantly enhanced in the Snail-overexpressing group. However, no significant differences were observed between the GEM and GEM + Snail OE groups. Moreover, the establishment of Snail-overexpressed cells was not as successful as expected. The relatively low transfection efficiency of the transfection reagent might be accountable for this. In future studies, a more successful establishment of Snail-overexpressed cells will be explored to verify the data achieved in the present study. In addition, further investigation need to be performed to explore the underlying molecular mechanism of the regulatory effect of Emo on the expression level of Snail, such as screening differentially expressed miRNAs by using gene chips.

In the present study, promising effects of Emo against GEM-resistance in pancreatic cancer were observed. However, in developing Emo as a drug, its limitations should be considered, including poor oral bioavailability (36) and rapid elimination (37). In further research, developing formulation methods to improve the oral bioavailability of Emo, such as introducing a solubility enhancer or crystallization inhibitor, is necessary. Furthermore, hepatotoxicity, nephrotoxicity and reproductive toxicity of Emo have been reported (38), which significantly limits the its further development as therapeutic drug. Further research is needed to investigate structure-function relationships to explore the potential of optimizing the structure of Emo to reduce off-target toxicity and maintain on-target activity.

The data from the present study revealed that Emo may reverse GEM-resistance in pancreatic cancer by suppressing stemness through the regulation of EMT progression (Fig. 8).

Acknowledgements

Not applicable.

Funding

The present study was supported by the Natural Science Foundation of Zhejiang Province (grant no. LQ20H310001).

Availability of data and materials

The datasets used and/or analyzed during the current study are available from the corresponding author on reasonable request.

Authors' contributions

JL and WW were responsible for the conception and design of the research. JW was responsible for the acquisition, analysis and interpretation of the data. YH performed the statistical analysis. JL obtained funding for the study. WW and SC drafted the manuscript. SC performed the experiments and revised the manuscript for important intellectual content. JL and WW confirm the authenticity of all the raw data. All authors have read and approved the final manuscript.

Ethics approval and consent to participate

All animal experiments performed in this study were authorized by the ethical committee of Zhejiang Cancer Hospital (approval no. 2019-07-006) and conducted according to the guidelines for care and use of laboratory animals and the principles of laboratory animal care and protection.

Patient consent for publication

Not applicable.

Competing interests

The authors declare that they have no competing interests.

References

1. Park W, Chawla A and O'Reilly EM: Pancreatic cancer: A review. JAMA 326: 851-862, 2021.
2. Sarvepalli D, Rashid MU, Rahman AU, Ullah W, Hussain I, Hasan B, Jehanzeb S, Khan AK, Jain AG, Khetpal N and Ahmad S: Gemcitabine: A review of chemoresistance in pancreatic cancer. Crit Rev Oncog 24: 199-212, 2019.
3. Wang L, Dong P, Wang W, Huang M and Tian B: Gemcitabine treatment causes resistance and malignancy of pancreatic cancer stem-like cells via induction of lncRNA HOTAIR. Exp Ther Med 14: 4773-4780, 2017.
4. de Sousa Cavalcante L and Monteiro G: Gemcitabine: Metabolism and molecular mechanisms of action, sensitivity and chemoresistance in pancreatic cancer. Eur J Pharmacol 741: 8-16, 2014.
5. Gangemi R, Paleari L, Orengo AM, Cesario A, Chessa L, Ferrini S and Russo P: Cancer stem cells: A new paradigm for understanding tumor growth and progression and drug resistance. Curr Med Chem 16: 1688-1703, 2009.
6. Du Z, Qin R, Wei C, Wang M, Shi C, Tian R and Peng C: Pancreatic cancer cells resistant to chemoradiotherapy rich in 'stem-cell-like' tumor cells. Dig Dis Sci 56: 741-750, 2011.
7. Li Y, Kong D, Ahmad A, Bao B and Sarkar FH: Pancreatic cancer stem cells: Emerging target for designing novel therapy. Cancer Lett 338: 94-100, 2013.
8. Abel EV and Simeone DM: Biology and clinical applications of pancreatic cancer stem cells. Gastroenterology 144: 1241-1248, 2013.
9. Sancho P, Alcala S, Usachov V, Hermann PC and Sainz B Jr: The ever-changing landscape of pancreatic cancer stem cells. Pancreatology 16: 489-496, 2016.
10. Reya T, Morrison SJ, Clarke MF and Weissman IL: Stem cells, cancer, and cancer stem cells. Nature 414: 105-111, 2001.
11. Shah AN, Summy JM, Zhang J, Park SI, Parikh NU and Gallick GE: Development and characterization of gemcitabine-resistant pancreatic tumor cells. Ann Surg Oncol 14: 3629-3637, 2007.
12. Lamouille S, Xu J and Derynck R: Molecular mechanisms of epithelial-mesenchymal transition. Nat Rev Mol Cell Biol 15: 178-196, 2014.
13. Iwatsuki M, Mimori K, Yokobori T, Ishi H, Beppu T, Nakamori S, Baba H and Mori M: Epithelial-mesenchymal transition in cancer development and its clinical significance. Cancer Sci 101: 293-299, 2010.
14. Mani SA, Guo W, Liao MJ, Eaton EN, Ayyanan A, Zhou AY, Brooks M, Reinhard F, Zhang CC, Shipitsin M, *et al*: The epithelial-mesenchymal transition generates cells with properties of stem cells. Cell 133: 704-715, 2008.
15. Babaei G, Aziz SG and Jaghi NZZ: EMT, cancer stem cells and autophagy; the three main axes of metastasis. Biomed Pharmacother 133: 110909, 2021.
16. Reiman JM, Knutson KL and Radisky DC: Immune promotion of epithelial-mesenchymal transition and generation of breast cancer stem cells. Cancer Res 70: 3005-3008, 2010.
17. Tian K, Zhang H, Chen X and Hu Z: Determination of five anthraquinones in medicinal plants by capillary zone electrophoresis with beta-cyclodextrin addition. J Chromatogr A 1123: 134-137, 2006.
18. Shrimali D, Shanmugam MK, Kumar AP, Zhang J, Tan BK, Ahn KS and Sethi G: Targeted abrogation of diverse signal transduction cascades by emodin for the treatment of inflammatory disorders and cancer. Cancer Lett 341: 139-149, 2013.
19. Li J, Liu P, Mao H, Wanga A and Zhang X: Emodin sensitizes paclitaxel-resistant human ovarian cancer cells to paclitaxel-induced apoptosis *in vitro*. Oncol Rep 21: 1605-1610, 2009.
20. Way TD, Huang JT, Chou CH, Huang CH, Yang MH and Ho CT: Emodin represses TWIST1-induced epithelial-mesenchymal transitions in head and neck squamous cell carcinoma cells by inhibiting the β-catenin and Akt pathways. Eur J Cancer 50: 366-378, 2014.
21. Thacker PC and Karunagaran D: Curcumin and emodin down-regulate TGF-β signaling pathway in human cervical cancer cells. PLoS One 10: e0120045, 2015.
22. Pooja T and Karunagaran D: Emodin suppresses Wnt signaling in human colorectal cancer cells SW480 and SW620. Eur J Pharmacol 742: 55-64, 2014.
23. Bai J, Wu J, Tang R, Sun C, Ji J, Yin Z, Ma G and Yang W: Emodin, a natural anthraquinone, suppresses liver cancer in vitro and in vivo by regulating $VEGFR_2$ and miR-34a. Invest New Drugs 38: 229-245, 2020.
24. Zeng S, Pöttler M, Lan B, Grützmann R, Pilarsky C and Yang H: Chemoresistance in pancreatic cancer. Int J Mol Sci 20: 4504, 2019.
25. Yin T, Wei H, Gou S, Shi P, Yang Z, Zhao G and Wang C: Cancer stem-like cells enriched in Panc-1 spheres possess increased migration ability and resistance to gemcitabine. Int J Mol Sci 12: 1595-1604, 2011.
26. Hermann PC, Huber SL, Herrler T, Aicher A, Ellwart JW, Guba M, Bruns CJ and Heeschen C: Distinct populations of cancer stem cells determine tumor growth and metastatic activity in human pancreatic cancer. Cell Stem Cell 1: 313-323, 2007.
27. Rao CV and Mohammed A: New insights into pancreatic cancer stem cells. World J Stem Cells 7: 547-555, 2015.
28. Izumiya M, Kabashima A, Higuchi H, Igarashi T, Sakai G, Iizuka H, Nakamura S, Adachi M, Hamamoto Y, Funakoshi S, *et al*: Chemoresistance is associated with cancer stem cell-like properties and epithelial-to-mesenchymal transition in pancreatic cancer cells. Anticancer Res 32: 3847-3853, 2012.
29. Rhim AD, Mirek ET, Aiello NM, Maitra A, Bailey JM, McAllister F, Reichert M, Beatty GL, Rustgi AK, Vonderheide RH, *et al*: EMT and dissemination precede pancreatic tumor formation. Cell 148: 349-361, 2012.
30. Voon DC, Wang H, Koo JK, Chai JH, Hor YT, Tan TZ, Chu YS, Mori S and Ito Y: EMT-induced stemness and tumorigenicity are fueled by the EGFR/Ras pathway. PLoS One 8: e70427, 2013.
31. Grau Y, Carteret C and Simpson P: Mutations and chromosomal rearrangements affecting the expression of snail, a gene involved in embryonic patterning in Drosophila melanogaster. Genetics 108: 347-360, 1984.
32. Cano A, Pérez-Moreno MA, Rodrigo I, Locascio A, Blanco MJ, del Barrio MG, Portillo F and Nieto MA: The transcription factor snail controls epithelial-mesenchymal transitions by repressing E-cadherin expression. Nat Cell Biol 2: 76-83, 2000.
33. Xiong Y, Wang Y, Wang L, Huang Y, Xu Y, Xu L, Guo Y, Lu J, Li X, Zhu M and Qian H: MicroRNA-30b targets Snail to impede epithelial-mesenchymal transition in pancreatic cancer stem cells. J Cancer 9: 2147-2159, 2018.
34. Wang H, Wang HS, Zhou BH, Li CL, Zhang F, Wang XF, Zhang G, Bu XZ, Cai SH and Du J: Epithelial-mesenchymal transition (EMT) induced by TNF-α requires AKT/GSK-3β-mediated stabilization of snail in colorectal cancer. PLoS One 8: e56664, 2013.
35. Hwang WL, Yang MH, Tsai ML, Lan HY, Su SH, Chang SC, Teng HW, Yang SH, Lan YT, Chiou SH and Wang HW: SNAIL regulates interleukin-8 expression, stem cell-like activity, and tumorigenicity of human colorectal carcinoma cells. Gastroenterology 141: 279-291, 291.e1-e5, 2011.
36. Liu W, Feng Q, Li Y, Ye L, Hu M and Liu Z: Coupling of UDP-glucuronosyltransferases and multidrug resistance-associated proteins is responsible for the intestinal disposition and poor bioavailability of emodin. Toxicol Appl Pharmacol 265: 316-324, 2012.
37. Chen J, Li S, Liu M, Lam CWK, Li Z, Xu X, Chen Z, Zhang W and Yao M: Bioconcentration and metabolism of emodin in zebrafish eleutheroembryos. Front Pharmacol 8: 453, 2017.
38. Dong X, Fu J, Yin X, Cao S, Li X, Lin L; Huyiligeqi and Ni J: Emodin: A review of its pharmacology, toxicity and pharmacokinetics. Phytother Res 30: 1207-1218, 2016.